THE MORPHOLOGY OF THE PROXIMAL FEMUR

A THREE-DIMENSIONAL RADIOGRAPHIC ANALYSIS

P. J. RUBIN, P. F. LEYVRAZ, J. M. AUBANIAC, J. N. ARGENSON, P. ESTÈVE, B. DE ROGUIN

From Lausanne Orthopaedic Hospital and Aix-Marseille University

Biological fixation of cementless femoral implants requires primary stability by optimal fit in the proximal femur. The anatomy of the bone must then be known precisely.

We analysed in vitro the accuracy of bone measurements of 32 femurs and compared the dimensions obtained from radiographs and CT scans with the true anatomical dimensions.

Standard radiographs gave only a rough approximation of femoral geometry (mean difference: 2.4 $\pm$ 1.4 mm) insufficiently accurate to allow selection of the best fitting prosthesis from a range of sizes and altogether inadequate to design a custom-made prosthesis.

CT scans give greater accuracy (mean difference: 0.8 $\pm$ 0.7 mm) in our experimental conditions, but in clinical practice additional sources of error exist.

The long-term complications of cemented total hip replacement, particularly the loosening rate of the femoral component (Amstutz 1970) have led to the development of implants with biological fixation (Morscher 1984; Engh and Bobyn 1985). In such implants, stable primary fixation of the components is mandatory to obtain bony ingrowth and secondary long-term stability (Zweymüller 1984; Walker et al 1987). Optimum filling of the proximal metaphysis by the implant is one way of assuring primary stable fixation and allowing physiological load transfer (Walker and Robertson 1988).

Because of the great variation of femoral anatomy in the normal population, precise bone–implant fit is difficult to achieve and there have been few detailed studies of the geometry of the femur. The only recent one is that of Noble et al (1988) based on anteroposterior and lateral radiographs. They classified the femoral shapes into three main groups, providing a basis for the design and selection of femoral implants. The new approach to three-dimensional imaging arose from the use of CT scans for the design of so-called custom-made prostheses (Aldinger and Weipert 1990; Essinger, Robertson and Esteve 1990). But all these techniques reflect only indirectly the true anatomical configuration. The question remains: to what extent do these methods reveal the reality of its three-dimensional femoral geometry?

We have compared the internal and external geometry of the proximal femur, as obtained from radiographs or CT scans, with actual measurements of anatomical specimens.

P. J. Rubin, MS, Research Engineer

P. F. Leyvraz, MD, PD, Orthopaedic Surgeon
B. de Roguin, MD, Orthopaedic Surgeon
Hôpital Orthopédique de la Suisse Romande, 4 avenue Pierre Decker, 1005 Lausanne, Switzerland.

J. M. Aubaniac, MD, Professor of Orthopaedics
J. N. Argenson, MD, Orthopaedic Surgeon
Aix-Marseille University, Service de Chirurgie Orthopédique, Hôtel Dieu, 13002 Marseille, France.

P. Estève, MD, Radiologist
Hôpital Ambroise-Paré, 1 rue d'Eylau, 13291 Marseille, France.

Correspondence should be sent to Dr P. J. Rubin.

0301-620X/92/1236 $2.00
J Bone Joint Surg [Br] 1992; 74-B: 28–32.

MATERIALS AND METHODS

We used 32 normal adult femurs (17 left and 15 right) obtained from cadavers. The bones were initially stored at −20°C. The donor population of 13 men and 19 women had died at an average age of 82 years (range 70 to 95). The bones were clamped in a jig aligned to a reproducible axis system based on the centre of the lesser trochanter and the isthmus of the femoral shaft (Fig. 1). Each femur was examined successively by radiography and CT scan, and was finally cut into slices for direct measurement.

Radiographic examination. Anteroposterior and lateral views were obtained for each specimen using a precise standardised technique.

Anteroposterior view. The femur was placed in a plexiglass box with parallel sides. The femur lay in neutral rotation. The distance between the X-ray source and the film was 1.2 m and the beam was centred on the lesser trochanter. *Lateral view.* Without moving the femur, the X-ray source was rotated through 90° in the vertical plane, the distance between the source and the film remaining the same.

Three radio-opaque markers placed on the femoral shaft allowed us to compensate for magnification. The radiographs were digitised on a video camera system connected to a microcomputer. The inner and outer contours of the bone were picked out manually and the internal and external geometry of the femur was then reconstructed in three dimensions.

We extracted ten periosteal and endosteal dimensions, as described by Noble et al (1988) from the anteroposterior view (Fig. 2). These values were then treated by a data processing program to correct magnification and distortion. The canal flare index (CFI), defined as the ratio of the intracortical width of the femur at a point 20 mm proximal to the lesser trochanter to that at the medullary isthmus, was calculated for each bone, allowing us to classify the femurs into three general shapes (normal, 'stovepipe' and 'champagne-flute').

CT scan examination. The bones were placed in water-filled plexiglass boxes in the same way as for the radiological examination and were centred in the CT scan field to minimise beam hardening and the partial volume effect. Axial slices, 1 mm thick, were taken every 5 mm from the superior pole of the femoral head to the midshaft. An interactive boundary detection program was used to determine the contours of the bone–water and the cortical–trabecular bone interfaces. The detection contour program used gradient and density techniques to improve the precision of the endosteal measurements in the proximal femur. These CT data were then processed to obtain three-dimensional reconstructions of the external and internal geometry.

Anatomical examination. The femurs were embedded in polyurethane foam and sectioned transversely parallel to the bicondylar plane. The sections were 2 mm thick and spaced every 5 mm. The slices were photographed with a video camera system and the contours were extracted using the same method as for CT scans. The anatomical data were then processed to obtain three-dimensional reconstructions of the external and internal geometry. The reconstructed femur generated from these measurements was taken as the reference.

In order to compare the anatomical geometry with

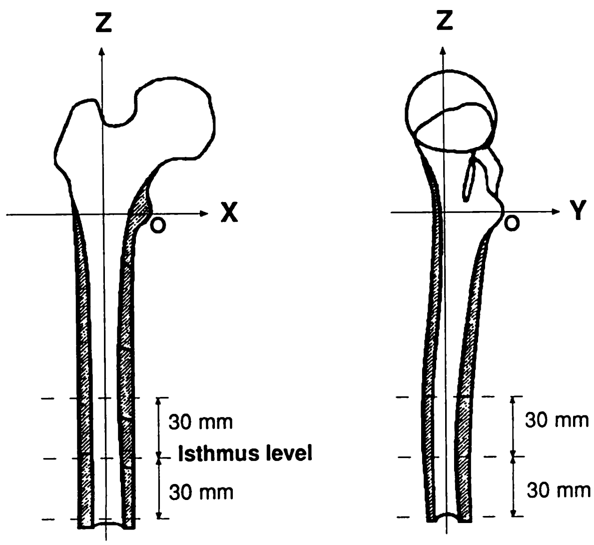

Fig. 1

Reference axis system
O: Centre of the lesser trochanter (origin of the axis system)
X: Horizontal axis through O on the anteroposterior view
Y: Horizontal axis through O on the lateral view
Z: Vertical axis through O on the anteroposterior and lateral views.

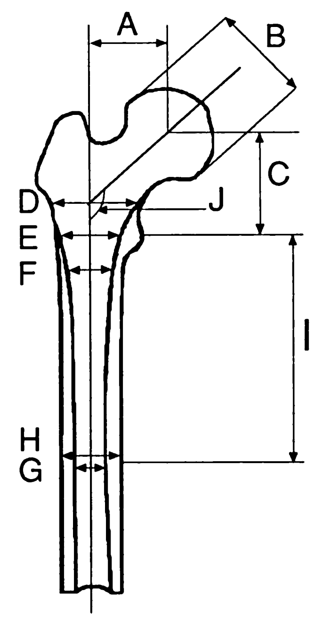

Fig. 2

Anatomical characteristics in millimetres measured on the anteroposterior radiograph.

A: Femoral head offset
B: Femoral head diameter
C: Femoral head position
D: Canal width, 20 mm above the lesser trochanter
E: Canal width, at the level of the lesser trochanter
F: Canal width, 20 mm below the lesser trochanter
G: Endosteal width at the isthmus
H: Periosteal width at the isthmus
I: Isthmus position
J: Neck–shaft angle (degrees).

the radiographic and CT scan reconstructions, we calculated an accuracy index ΔR. This index was defined as the difference between a radius of the anatomical section and the same radius for the corresponding section measured radiographically or on the CT scan (Fig. 3).

RESULTS

Two-dimensional measurements. The mean value for each parameter measured on the standard anteroposterior radiographs are given in Table I, from which are extracted canal flare indices (Fig. 4).

Three-dimensional reconstruction of the femoral geometry. The mean internal and external radii of all femurs measured from the radiographs at the distal and proximal zones, with maximum and minimum values and the standard deviation, are given in Table II. Similar measurements from the CT scans are shown in Table III. The distal zone is defined as the part below the lesser trochanter and the proximal zone as the part above the lesser trochanter.

Figure 5 illustrates the accuracy of the reconstruction by both methods for one femur.

DISCUSSION

The two-dimensional measurements reported in this study are very similar to those published by Noble et al (1988). As to the canal flare index (Fig. 4), our distribution (CFI = 3.36 $\pm$ 0.75) was approximately the same as theirs (CFI = 3.8 $\pm$ 0.74). The only difference was a shift of the curve to the left. This is probably due to the fact that on average our donor population was older and consequently the average isthmus diameter of our specimens was greater, confirming previous anthropological studies (Smith and Walker 1964; Ericksen 1979; Ruff and Hayes 1984), which have demonstrated the strong correlation between the widening of the canal and the age of the femur.

This has several consequences for the long-term function of cementless total hip arthroplasty especially in young patients. The stability of the femoral component depends on a balance of proximal and distal load transfer from the implant to the femur (Huiskes 1980). The relative contributions of this proximal and distal support depend mainly on the fit of the prosthesis to the bone. A close intramedullary stem fit decreases the stresses at the proximal implant–bone interface. But if the medullary canal expands with increasing age, medial migration of the prosthesis may occur with possible mechanical loosening and subsidence of the implant.

In the distal zone, standard radiographs provide an acceptable level of accuracy for clinical use, but proximally they are inaccurate. Their imprecision is increased in clinical practice by other factors. Correct positioning of the patient may be difficult because of pain or contracture, and small variations in leg rotation signifi-

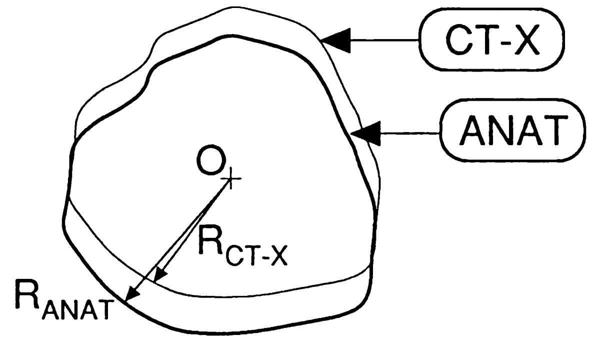

Fig. 3

The index of accuracy (ΔR) demonstrated on one transverse section
CT–X: section derived from radiograph or CT scan
ANAT: section derived from anatomical measurements
O: Centre of gravity (anatomic reference)
R_{CT-X}: radius of the radiographic or CT scan section
R_{ANAT}: radius of the anatomical section.
The index of accuracy (ΔR) = R_{CT-X} R_{ANAT}.

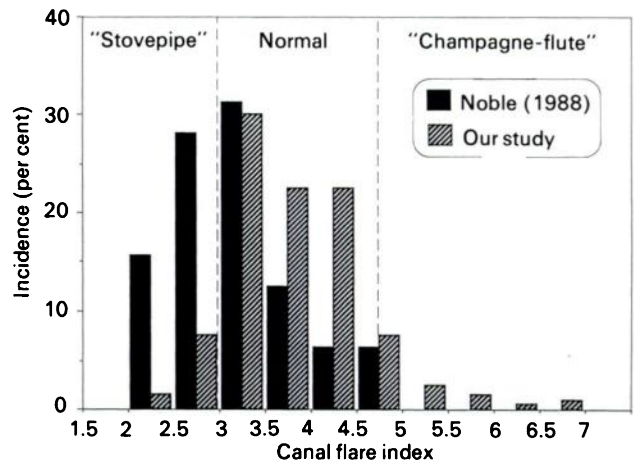

Fig. 4

Distribution of canal flare indices compared with those obtained by Noble (1988).

Table I. Mean values of guidelines measured on the anteroposterior radiographs

Dimensions (millimetres)	Mean	SD	Range
Femoral length	443.6	21.8	402.0 to 486.0
Femoral head offset	47.0	7.2	33.2 to 62.8
Femoral head diameter	43.4	2.6	39.3 to 48.3
Femoral head position	56.1	8.2	35.8 to 70.2
Canal width (lesser trochanter + 20)	43.1	5.0	35.8 to 51.3
Canal width (lesser trochanter)	27.9	3.6	23.0 to 35.9
Canal width (lesser trochanter – 20)	21.0	2.7	17.3 to 26.4
Endosteal width at the isthmus level	13.1	2.1	9.1 to 18.3
Periosteal width at the isthmus level	26.7	1.8	23.1 to 31.9
Isthmus position	105.7	17.9	82.0 to 160.0
Neck–shaft angle (degrees)	122.9	7.6	100.7 to 137.8
Canal flare index	3.36	0.75	2.37 to 5.35

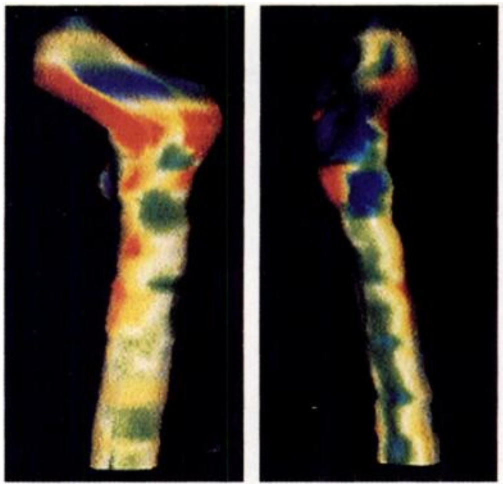

Fig. 5a

ΔR for radiographic reconstruction of the external geometry.

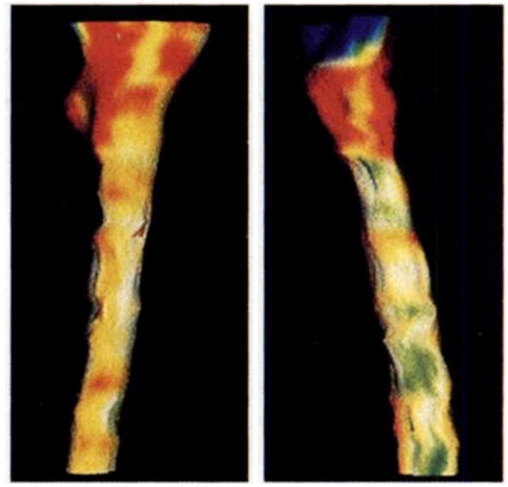

Fig. 5b

ΔR for radiographic reconstruction of the internal geometry.

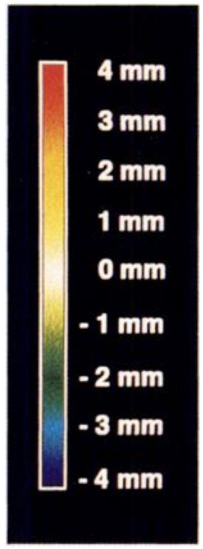

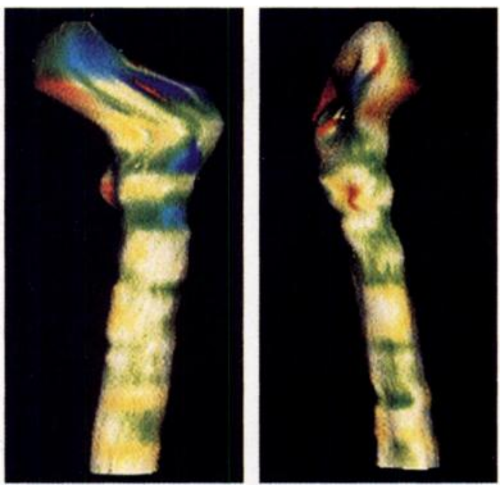

Fig. 5c

ΔR for CT scan reconstruction of the external geometry.

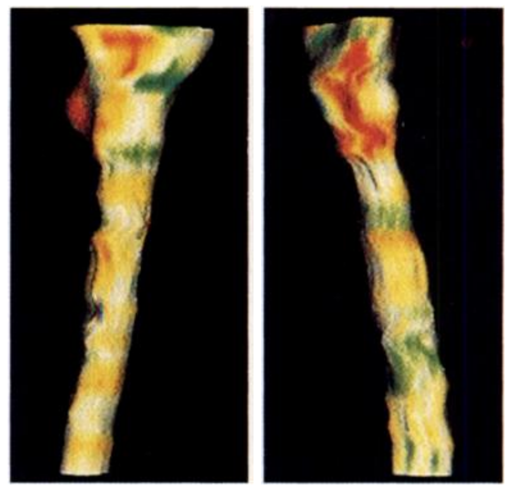

Fig. 5d

ΔR for CT scan reconstruction of the internal geometry.

The index of accuracy (ΔR) demonstrated visually on one specimen by a colour scale. When the radii are closely similar the surface appears white and when they are different, positive or negative, the surface appears red or blue, respectively. In each pair of pictures the anteroposterior image is on the left and the lateral on the right.

Table II. Index of accuracy (ΔR in mm) of radiographic measurements of 32 femurs

	Internal radius			External radius		
Level in femur*	Mean	SD	Range	Mean	SD	Range
Proximal	2.4	1.4	6.1 to 0.5	2.5	1.9	7.2 to 0.8
Distal	1.3	0.4	1.8 to 0.2	1.1	0.4	1.8 to 0.1

*see text

Table III. Index of accuracy (ΔR in mm) of CT scan measurements of 32 femurs

	Internal radius			External radius		
Level in femur*	Mean	SD	Range	Mean	SD	Range
Proximal	0.9	0.4	1.5 to 0.1	0.8	0.4	1.5 to 0.2
Distal	0.8	0.4	1.2 to 0.1	0.7	0.3	1.1 to 0

*see text

cantly alter some of the dimensions, such as neck–shaft angle, calcar curvature, and isthmus width (Rubin, Levyraz and Heegaard 1989).

Experimental and clinical studies have all emphasised the importance of accurate cross-sectional fit to achieve stability and good load transfer (Poss et al 1988; Walker and Robertson 1988). Radiographic measurements are inadequate for this purpose.

The limitations of standard radiology are most obvious in the pre-operative planning of cementless or custom-made prostheses. Radiographs can only provide a rough approximation to the real size and shape of the femoral component which will fit most precisely. The final, and probably the most accurate determination of the appropriate component, must therefore be made during the surgical procedure. If we consider two cementless off-the-shelf prostheses on the market, the PCA (Howmedica Inc, Rutherford, New Jersey) and the CLS (Protek Inc, Berne, Switzerland), and look at the extensive range of frontal widths at the proximal level, we find, for the seven sizes of PCA stem, that the variation between one size and the next is from 0.8 to 2.2 mm; in the CLS, the changes in widths vary from 0.9 to 1.3 mm. Our results show that radiographic accuracy in measuring the proximal region is 2.4 mm $\pm$ 1.4 mm. Consequently radiograph analysis at best allows an appreciation within three sizes.

The CT scan is an accurate technique when used in experimental conditions, as shown by our results but in clinical practice it is not error-free. The amount of error has been estimated to vary from 10% to 40% (Robertson and Huang 1986), the main errors arising from beam hardening and the partial volume effect (Capello 1989). Another source of error is patient movement during the examination. Furthermore, CT scan equipment, both the source and the detector, deteriorate with time. If we take account of all these theoretical errors, we can calculate from our in vitro measurements a mean index of accuracy for both zones (proximal and distal) of $\Delta R = 0.8$ mm ($\pm$ 0.7 mm). The worst possible error is 1.5 mm which is hardly acceptable in the planning of custom-made prostheses nor even in the choice of an off-the-shelf implant. These errors can be minimised to some extent by using calibration phantoms and/or second-order correction algorithms. However, another difficulty remains, that of defining the border between cortical and cancellous bone in the proximal zone where the cortex is very thin.

We conclude from our study that the CT scan is a precise technique in experimental conditions and that its accuracy remains adequate in the clinical situation when care is taken to limit technical imprecisions. But it is an expensive investigation which is not always easily available to the surgeon. In routine total hip replacement, conventional radiology remains the most convenient method available. However, in the absence of a precise radiological protocol, radiographic measurements are insufficiently accurate to allow the pre-operative design of custom-made prostheses. Radiological accuracy could be improved in the future by computerised correction of radiological femoral dimensions through the availability of large banks of anatomical or CT scan-generated three-dimensional data.

The authors would like to thank Symbios Orthopedie for their Medical Image processing software.

No benefits in any form have been received or will be received from a commercial party related directly or indirectly to the subject of this article.

REFERENCES

Aldinger G, Weipert A. Designing principles of custom-made hip stems. Proc 3rd annual symposium on custom-made prostheses, Nice, 1990.

Amstutz HC. Complications of total hip replacement. *Clin Orthop* 1970; 72:123-37.

Capello WN. Fit the patient to the prosthesis: an argument against the routine use of custom hip implants. *Clin Orthop* 1989; 249:56-9.

Engh CA, Bobyn JD. *Biological fixation in total hip arthroplasty.* New Jersey: Slack Inc, 1985.

Ericksen MF. Aging changes in the medullary cavity of the proximal femur in American Blacks and Whites. *Am J Phys Anthropol* 1979; 51:563-9.

Essinger JR, Robertson DD, Esteve P. Evaluation of CT accuracy for custom prostheses designing. Proc 3rd annual symposium on custom-made prostheses, Nice, 1990.

Huiskes R. Some fundamental aspects of human joint replacement: analyses of stresses and heat conduction in bone-prosthesis structures. *Acta Orthop Scand* 1980:Suppl 185.

Morscher E, ed. *The cementless fixation of hip endoprostheses.* Berlin, etc: Springer-Verlag, 1984.

Noble PC, Alexander JW, Lindahl LJ, et al. The anatomic basis of femoral component design. *Clin Orthop* 1988; 235:148-65.

Poss R, Walker P, Spector M, et al. Strategies for improving fixation of femoral components in total hip arthroplasty. *Clin Orthop* 1988; 235:181-94.

Robertson DD Jr, Huang HK. Quantitative bone measurements using X-ray computed tomography with second-order correction. *Med Phys* 1986; 13:474-9.

Rubin PJ, Leyvraz PF, Heegaard JH. Radiological variations in the anatomical parameters of the proximal femur in relation to rotation. *French J Orthop Surg* 1989; 3:121-7.

Ruff CB, Hayes WC. Age changes in geometry and mineral content of the lower limb bones. *Ann Biomed Eng* 1984; 12:573-84.

Smith RW, Walker RR. Femoral expansion in aging women: implications for osteoporosis and fractures. *Science* 1964; 145: 156-7.

Walker PS, Robertson DD. Design and fabrication of cementless hip stems. *Clin Orthop* 1988; 235:25-34.

Walker PS, Schneeweis, Murphy S, Nelson P. Strain and micromotions of press-fit femoral stem prostheses. *J Biomech* 1987; 20:693-702.

Zweymüller K. First clinical experience with an uncemented modular femoral prosthesis system with a wrought Ti-6Al-4V stem and an Al_2O_3 ceramic head. In: Morscher E, ed. *The cementless fixation of hip endoprostheses.* Berlin: Springer-Verlag, 1984; 150-5.